E-ISSN: 3050-9459
Journal of Ophthalmology and Advance Research

ATHENAEUM SCIENTIFIC PUBLISHERS

Research Article

Improving Glaucoma Diagnosis with Multimodal Analysis Using Optical Coherence Tomography Angiography

Haafiz Hashim[1], Haris Hashim[2], Karanjit Kooner[1,3*]

[1]University of Texas Southwestern Medical Center, 5323 Harry Hines Blvd, Dallas, TX 75390, USA

[2]University of Texas at Dallas, 800 W Campbell Rd, Richardson, TX 75080, USA

[3]VA North Texas Health Care System, 4500 S Lancaster Rd, Dallas, TX, 75216, USA

***Correspondence author:** Karanjit S Kooner, MD, Department of Ophthalmology, University of Texas Southwestern Medical Center 5323 Harry Hines Blvd, Dallas, TX 75390-9057, USA; Email: Karanjit.Kooner@UTSouthwestern.edu

Citation: Hashim H, et al. Improving Glaucoma Diagnosis with Multimodal Analysis Using Optical Coherence Tomography Angiography. J Ophthalmol Adv Res. 2025;6(3):1-11.

https://doi.org/10.46889/JOAR.2025.6309

Received Date: 23-09-2025

Accepted Date: 19-10-2025

Published Date: 26-10-2025

Abstract

Purpose: To assess the role of multimodal Optical Coherence Tomography Angiography (OCTA) analysis in glaucoma diagnosis.

Methods: This Institutional Review Board (IRB) approved, retrospective, single academic center study consisted of 357 patients (635 eyes), including 193 healthy, 99 Ocular Hypertension (OHT), 128 open angle Glaucoma Suspect (GS) and 215 POAG eyes. The following clinical data was collected for all patients: Retinal Nerve Fiber Layer Thickness (RNFL), Cup/Disc Ratio (CDR), Central Corneal Thickness (CCT) and history of myopia, hyperopia, Hypertension (HTN), Diabetes (DM) and Cardiovascular Disease (CVD). OCTA scans of the optic nerve head and macula were analyzed using Open-Source Software (OpenCV), calculating Vessel Density (VD), Vessel Length Density (VLD) and fractal dimension (FD). The data was divided into a training and testing set. Using the training data, we created five diagnostic models (demographic, VD-FD, VLD-FD, clinical and multimodal). We calculated Receiver Operating Curves (ROC) using the testing data and compared the models using Area Under the Curve (AUC) analysis.

Results: VD, VLD and FD were significantly reduced in the POAG group ($p < 0.0001$). The multimodal model performed the best (AUC = 0.898), followed by the clinical model (AUC = 0.888), the VD-FD model (AUC = 0.780), the VLD-FD model (AUC = 0.774) and the demographic model (AUC = 0.741). The multimodal model performed significantly better than all other models ($p = 0.035$).

Conclusion: Our analysis indicates that diagnosing glaucoma with a multimodal approach utilizing OCTA is superior to using clinical and structural data alone.

Keywords: Glaucoma; Optical Coherence Tomography Angiography; Myopia; Hyperopia; Hypertension

Introduction

Primary Open Angle Glaucoma (POAG) is a multifactorial progressive glaucomatous optic neuropathy and the second most common cause of blindness worldwide [1,2]. The disease is characterized by chronic degeneration of the Retinal Ganglion Cells (RGCs), resulting in irreversible vision loss [3]. There are two primary theories of glaucoma pathophysiology: the mechanical theory states that increased Intraocular Pressure (IOP) directly damages the retinal nerve fibers at the level of the lamina cribrosa, while the vascular theory asserts that microvascular ischemia plays a substantial role [2,4-7]. Glaucoma diagnosis is a complex process and involves careful consideration of demographic, clinical and structural factors. Recently, Retinal Nerve Fiber Layer thickness (RNFL) has demonstrated especially strong discriminatory ability, playing a central role in the diagnosis of POAG [8]. Optical Coherence Tomography Angiography (OCTA) is a non-invasive imaging technology that provides detailed, replicable three-dimensional images of both the structural and microvascular components of the retina [9,10]. It provides a new dimension

in glaucoma diagnosis by quantifying Vessel Density (VD), defined as the total percentage of imaged area covered by vasculature [11]. Research has shown that glaucoma causes reductions in both macular and peripapillary VD; the latter has been found to be closely related to RNFL changes [9,10,12-16].

In addition to VD, a handful of studies have explored alternative OCTA metrics such as Vessel Length Density (VLD) and Fractal Dimension (FD). VLD is an alternative to VD which is theorized to be more sensitive to microvascular changes in capillaries and small vessels, while FD quantifies the branching, complexity and density of the microvascular network [11,17]. Both VLD and FD have demonstrated good ability to diagnose POAG, especially when combined with VD [11,18-20]. However, projects evaluating these alternative parameters have been limited by low sample sizes and homogenous patient populations [11,18-21]. Furthermore, most studies examining VLD and FD have included POAG and healthy groups, whereas borderline populations such as Glaucoma Suspects (GS) and Ocular Hypertension (OHT) have not been studied in detail [20,22,23].

Thus, the purpose of our study was to evaluate OCTA VD, VLD and FD in a large, heterogenous North Texas population consisting of healthy, POAG, GS and OHT patients, including their ocular and demographic variables. We hypothesize that combining these OCTA metrics with clinical and structural data would result in more accurate glaucoma diagnosis.

Materials and Methods

Study Population

This Institutional Review Board (IRB) approved, retrospective, cross-sectional study was conducted at the University of Texas Southwestern (UTSW) Medical Center. We adhered to the ethical principles described in the Declaration of Helsinki as well as the privacy standards outlined in the 1996 Health Insurance Portability and Accountability Act. Informed consent was not obtained due to the retrospective nature of the study, which did not require direct patient interaction.

The study population reviewed the electronic medical records of 478 consecutive patients seen at a UTSW tertiary care ophthalmology clinic between January 2020 and March 2023. All patients had undergone a full ophthalmologic exam, including visual acuity, automated visual field exam (24-2 Humphrey Field Analyzer, Carl Zeiss, Inc.), dilated fundus imaging, gonioscopy, Goldman applanation tonometry and OCTA imaging.

We included in our study population all patients over the age of 18 with open angles on gonioscopy. Exclusion criteria were moderate to severe myopia or hyperopia (defined as spherical equivalent > 3 diopters), secondary or angle closure glaucoma, severe vitreoretinal disease, previous optic neuropathy, ocular trauma and Alzheimer's disease, dementia or stroke. Patients with Image Quality Index < 4 or signal strength index (SSI) < 45 were also excluded.

Healthy individuals were defined as those with normal optic discs on fundoscopy without Visual Field Defects (VFD) or elevated intraocular pressure (IOP > 21 mmHg). Patients with POAG had characteristic glaucomatous optic disc changes (increased vertical disc cupping, thinning of the neuroretinal rim, notching, disc hemorrhages, displacement of retinal vessels) combined with corresponding VFD with or without elevated IOP. Glaucoma suspects included those with suspicious optic disc changes without corresponding VFD [24]. OHT patients were defined as those with chronically elevated IOP without optic disc changes or VFD. We included both eyes and analyzed them separately.

Data Acquisition

After defining our study population, a thorough chart review was conducted to gather the following demographic, clinical and ocular data: age, gender, race, ethnicity, family history of glaucoma, history of Hypertension (HTN), Diabetes (DM) or Cardiovascular Disease (CVD, defined here as coronary artery disease, peripheral arterial disease or congestive heart failure), IOP, RNFL and Cup/Disc Ratio (CDR).

Image Acquisition

OCTA imaging was obtained by the RTVue XR Avanti imaging system (Visionix Inc) using the built-in AngioVue imaging software version 2018.1.1.69. Each patient underwent a 3 × 3 mm macular scan centered on the fovea and a 4.5 × 4.5 mm scan centered on the Optic Nerve Head (ONH) as seen in Fig. 1. Optimal centering was performed with the aid of DualTrac Motion

Correction (DTMC) to minimize decentration and motion artifacts. For the macula, the OCTA scanner defines the superficial capillary plexus (Fig. 1) as the Inner Limiting Membrane (ILM) to 10 microns superficial to the Inner Plexiform Layer (IPL) and the deep capillary plexus (Fig. 1) as 10 microns superficial to the IPL to 10 microns deep to the Outer Plexiform Layer (OPL). For the ONH, the radial peripapillary capillary layer (RPC, Fig. 1) was defined as the ILM to the deep boundary of the RNFL layer in a 3.45 mm diameter circle centered on the ONH.

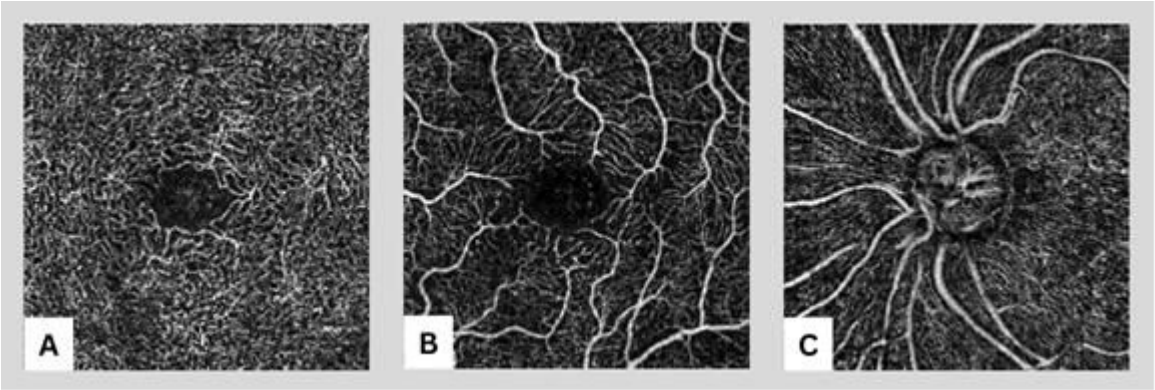

Figure 1: OCTA scan layers. Examples of analyzed OCTA scans are illustrated above, including scans of the deep capillary plexus (A), superficial capillary plexus (B) and radial peripapillary capillaries (C).

Image Processing and Quantification

We calculated VD, VLD and FD for each scan as depicted in Fig. 2. For image analysis, we utilized OpenCV, an open-source computer vision software library written in the Python programming language. Following import of OCTA images (Fig. 2), a global thresholding algorithm (Otsu) was applied, separating the pixels into background (0, black) and vessels (255, white) based on each pixel's value relative to a numerical threshold (Fig. 1). Otsu's thresholding algorithm is a built-in function of OpenCV designed to maximize inter-class variance and minimize intra-class variance [25]. Next, we calculated VD from the resulting binary images (Fig. 2) by determining the proportion of pixels that constituted vessels.

We then applied OpenCV's built-in skeletonization algorithm to convert the vasculature into 1-pixel-wide skeletonized vessel maps (Fig. 2). These vessel maps were used to compute VLD, defined as the ratio of the skeletonized vasculature length to the total image area.

Finally, we created a custom function to calculate the FD of the skeletonized vessel maps using the box-counting algorithm (Fig. 2). This method efficiently estimates FD by splitting an image into different sized grids and counting how many of the grid boxes (N) include part of the vascular pattern. As this process is repeated for smaller and smaller grid sizes, FD is approximately equivalent to the slope of the ratio between the logarithm of N (y-axis, Fig. 2) and the inverse of the grid size (x-axis, Fig. 2) [26]. We tested our function by comparing our calculated FD values to the open source software ImageJ, which has its own function to calculate fractal dimension.

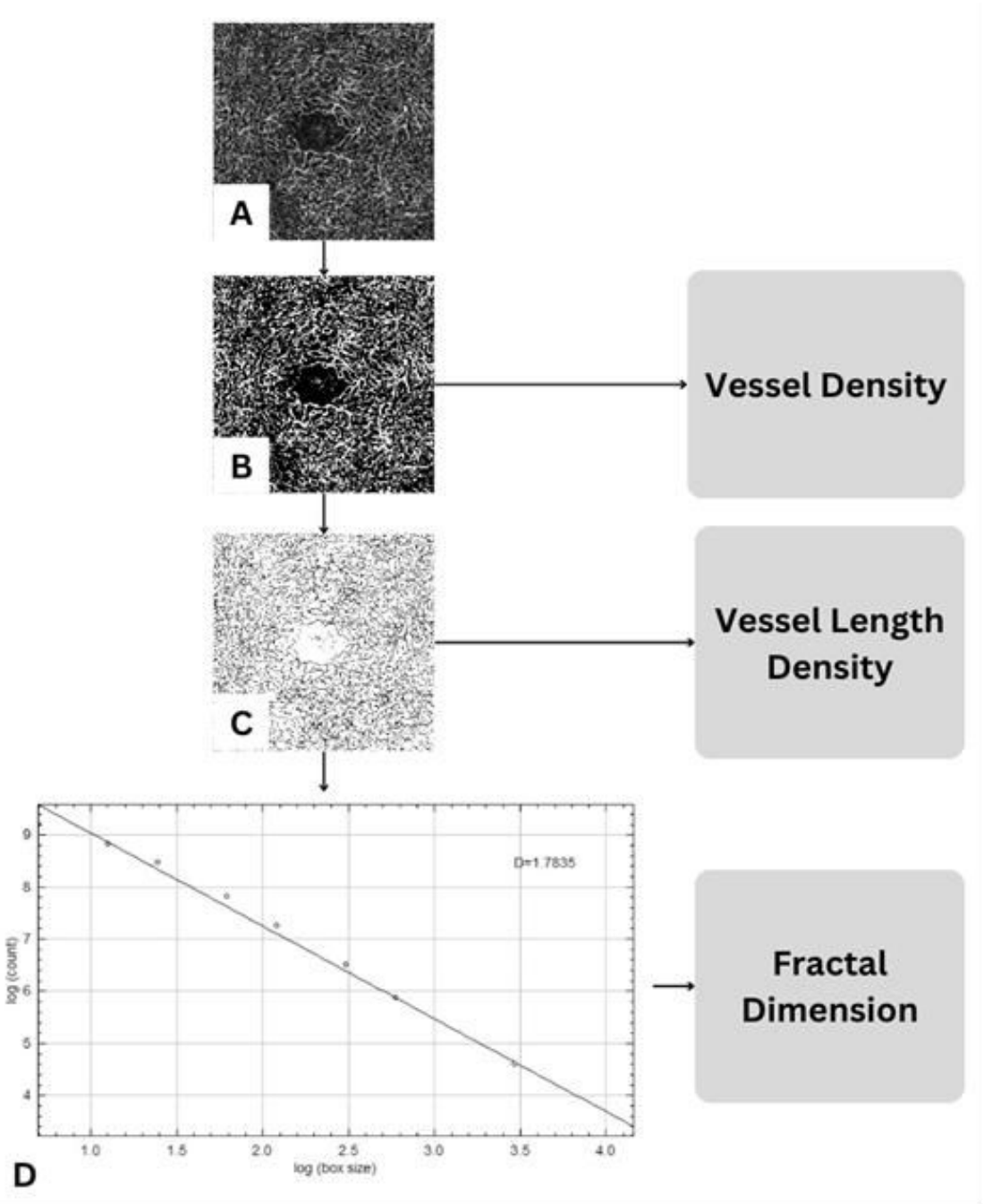

Figure 2: OCTA image processing steps. Image processing steps are depicted above in Fig. 2. First, the raw OCTA image (A) is converted to a black-and-white binary map (B). This binary map is used to calculate vessel density and then skeletonized (C). The skeletonized map is used to calculate vessel length density. Finally, the box-counting algorithm (D) is used to calculate the fractal dimension.

Exploratory Statistical Analysis

After analyzing images, exploratory statistical analysis was performed for all variables. One-way ANOVA was used to compare normally distributed continuous variables (CCT, CDR and macular SSI) between diagnosis groups (healthy, OHT, GS, POAG), while Student's t-test was used to compare between outcome groups (POAG or non-POAG). Similarly, the Kruskal-Wallis test was used to compare non-normally-distributed continuous variables (age, RNFL, GCC, VD, VLD, FD and disc SSI) between diagnosis groups while the Mann-Whitney U test was used to compare between outcome groups. The chi-squared test was used to compare categorical variables: sex, race, ethnicity, HTN, DM, CVD, myopia, hyperopia and the eye studied. A two-tailed significance threshold of $p = 0.05$ was chosen for this analysis.

Regression Models

Following exploratory analysis, we developed diagnostic models for different categories of data. To compare the highly correlated OCTA variables, we utilized Least Absolute Shrinkage and Selection Operator, also known as LASSO regression. Because this technique includes only the most significant predictors in the final diagnostic model, LASSO regression is a powerful tool for understanding glaucoma diagnosis.

Five different models were created to compare different categories of data: clinical, demographic, VD-FD, VLD-FD and multimodal (including clinical, demographic and OCTA data except VLD). The clinical model consisted of all clinical data, namely RNFL, GCC, CDR, CCT, history of mild myopia/hyperopia, HTN, DM and CVD. The demographic model included age, race, sex and ethnicity. The high correlation between VD and VLD made the OCTA models highly unstable; therefore, we divided the OCTA data into three models: VD-FD, VLD-FD and multimodal. As LASSO regression can only predict a binary response variable (POAG or non-POAG), the healthy, OHT and GS groups were combined into a non-POAG group for testing purposes. Model effectiveness was tested using Area Under the Curve (AUC) analysis and compared using DeLong's test.

Results

Out of 478 patients, we selected 105 healthy (193 eyes), 53 OHT (99 eyes), 77 GS (128 eyes) and 122 POAG (215 eyes) patients based on our inclusion and exclusion criteria. Exploratory analysis found significant differences between groups for age, sex, race, ethnicity, HTN, DM, CVD, RNFL, CDR, GCC, CCT, hyperopia, retina SSI and disc SSI (Table 1).

Variables	**POAG n = 215 (%)**	**OHT n = 99 (%)**	**GS n = 128 (%)**	**Healthy n = 193 (%)**	***p-Value***
Eye Studied					0.914
Left	101 (47.0%)	50 (50.5%)	64 (50.0%)	206 (49.0%)	
Right	114 (53.0%)	49 (49.5%)	64 (50.0%)	214 (51.0%)	
Age	71.21 ± 10.42	62.83 ± 12.52	64.14 ± 12.98	61.35 ± 12.46	*< 0.001*
Sex					*< 0.001*
Male	100 (46.5%)	30 (30.3%)	36 (28.1%)	128 (30.5%)	
Female	115 (53.5%)	69 (69.7%)	92 (71.9%)	292 (69.5%)	
Race					*< 0.001*
White	76 (35.3%)	48 (48.5%)	59 (46.1%)	191 (45.5%)	
Black	107 (49.8%)	29 (29.3%)	48 (37.5%)	117 (27.9%)	
South Asian	19 (8.8%)	16 (16.2%)	18 (14.1%)	74 (17.6%)	
East Asian	5 (2.3%)	2 (2.0%)	3 (2.3%)	30 (7.1%)	
Unknown	8 (3.7%)	4 (4.0%)	0 (0.0%)	8 (1.9%)	
Ethnicity					*0.001*
Hispanic	15 (7.0%)	20 (20.2%)	13 (10.2%)	47 (11.2%)	
Not Hispanic	190 (88.4%)	77 (77.8%)	115 (89.8%)	366 (87.1%)	
Unknown	10 (4.7%)	2 (2.0%)	0 (0.0%)	7 (1.7%)	
Coexisting Morbidities					
Hypertension					*0.009*
Yes	137 (63.7%)	66 (66.7%)	74 (57.8%)	237 (56.4%)	
No	76 (35.3%)	32 (32.3%)	54 (42.2%)	182 (43.3%)	
Unknown	2 (0.9%)	1 (1.0%)	0 (0.0%)	1 (0.2%)	
Diabetes Mellitus					*0.02*
Yes	65 (30.2%)	46 (46.5%)	39 (30.5%)	146 (34.8%)	
No	150 (69.8%)	52 (52.5%)	89 (69.5%)	273 (65.0%)	
Unknown	0 (0.0%)	1 (1.0%)	0 (0.0%)	1 (0.2%)	
Cardiovascular					*< 0.001*

Disease					
Yes	135 (62.8%)	67 (67.7%)	74 (57.8%)	225 (53.6%)	
No	80 (37.2%)	31 (31.3%)	54 (42.2%)	194 (46.2%)	
Unknown	0 (0.0%)	1 (1.0%)	0 (0.0%)	1 (0.2%)	
Clinical Metrics					
RNFL	75.14 ± 17.22	97.16 ± 9.17	91.65 ± 11.18	96.06 ± 9.52	*< 0.001*
CDR	0.60 ± 0.18	0.42 ± 0.19	0.46 ± 0.15	0.43 ± 0.17	*< 0.001*
GCC	79.8 ± 15.3	93.4 ± 7.0	88.9 ± 11.6	92.2 ± 9.7	*< 0.001*
CCT	532.5 ± 41.6	555.3 ± 32.2	548.4 ± 37.7	548.9 ± 38.8	*< 0.001*
Myopia					0.205
Yes	92 (42.8%)	33 (33.3%)	60 (46.9%)	170 (40.5%)	
No	123 (57.2%)	66 (66.7%)	68 (53.1%)	250 (59.5%)	
Hyperopia					*0.007*
Yes	37 (17.2%)	30 (30.3%)	34 (26.6%)	124 (29.5%)	
No	178 (82.8%)	69 (69.7%)	94 (73.4%)	296 (70.5%)	
Retina SSI	61.73 ± 6.57	64.68 ± 7.98	66.01 ± 7.22	65.82 ± 7.37	*< 0.001*
Disc SSI	57.64 ± 6.87	61.10 ± 7.84	62.69 ± 8.60	63.13 ± 8.41	*< 0.001*

Table 1: Characteristics of study participants, by diagnosis.

Healthy, GS and OHT eyes were combined into the non-POAG outcome group (420 eyes total). Significant differences were found between POAG and non-POAG eyes for age, sex, race, ethnicity, CVD, RNFL, CDR, GCC, CCT, hyperopia, retina SSI and disc SSI (Table 2).

Variables	**POAG n = 215 (%)**	**Non-POAG n = 420 (%)**	***p-Value***
Eye Studied			0.682
Left	101 (47.0%)	206 (49.0%)	
Right	114 (53.0%)	214 (51.0%)	
Age	71.21 ± 10.42	61.35 ± 12.46	*< 0.001*
Sex			*< 0.001*
Male	100 (46.5%)	128 (30.5%)	
Female	115 (53.5%)	292 (69.5%)	
Race			*< 0.001*
White	76 (35.3%)	191 (45.5%)	
Black	107 (49.8%)	117 (27.9%)	
South Asian	19 (8.8%)	74 (17.6%)	
East Asian	5 (2.3%)	30 (7.1%)	
Unknown	8 (3.7%)	8 (1.9%)	
Ethnicity			*0.025*
Hispanic	15 (7.0%)	47 (11.2%)	
Not Hispanic	190 (88.4%)	366 (87.1%)	
Unknown	10 (4.7%)	7 (1.7%)	
Coexisting Morbidities			
Hypertension			0.074
Yes	137 (63.7%)	237 (56.4%)	
No	76 (35.3%)	182 (43.3%)	
Unknown	2 (0.9%)	1 (0.2%)	
Diabetes Mellitus			0.281

Yes	65 (30.2%)	146 (34.8%)	
No	150 (69.8%)	273 (65.0%)	
Unknown	0 (0.0%)	1 (0.2%)	
Cardiovascular Disease			*0.0355*
Yes	135 (62.8%)	225 (53.6%)	
No	80 (37.2%)	194 (46.2%)	
Unknown	0 (0.0%)	1 (0.2%)	
Clinical Metrics			
RNFL	75.14 ± 17.22	96.06 ± 9.52	*< 0.001*
CDR	0.60 ± 0.18	0.43 ± 0.17	*< 0.001*
GCC	79.8 ± 15.3	92.2 ± 9.7	*< 0.001*
CCT	532.5 ± 41.6	548.9 ± 38.8	*< 0.001*
Myopia			0.635
Yes	92 (42.8%)	170 (40.5%)	
No	123 (57.2%)	250 (59.5%)	
Hyperopia			*< 0.001*
Yes	37 (17.2%)	124 (29.5%)	
No	178 (82.8%)	296 (70.5%)	
Retina SSI	61.73 ± 6.57	65.82 ± 7.37	*< 0.001*
Disc SSI	57.64 ± 6.87	63.13 ± 8.41	*< 0.001*

Table 2: Characteristics of study participants, POAG vs Non-POAG.

VD, VLD and FD were compared between POAG and non-POAG groups, summarized in Table 3. Significant differences were found between POAG and non-POAG for all three parameters (VD, VLD and FD) in every scan layer ($p < 0.001$).

Layer	OCTA Variable	POAG	Non-POAG	*p*-value
Superficial Macula	VD	0.188 ± 0.030	0.207 ± 0.043	<0.001
	VLD	0.054 ± 0.010	0.061 ± 0.013	<0.001
	FD	1.337 ± 0.067	1.381 ± 0.078	<0.001
Deep Macula	VD	0.265 ± 0.099	0.325 ± 0.101	<0.001
	VLD	0.074 ± 0.029	0.093 ± 0.031	<0.001
	FD	1.431 ± 0.140	1.511 ± 0.127	<0.001
Radial Peripapillary Capillaries	VD	0.174 ± 0.027	0.202 ± 0.033	<0.001
	VLD	0. 039 ± 0.006	0.046 ± 0.007	<0.001
	FD	1.237 ± 0.059	1.294 ± 0.054	<0.001

Table 3: OCTA variables, POAG vs non-POAG.

Based on LASSO regression, we designed five diagnostic models to differentiate POAG from non-POAG eyes (Table 4). Notably, FD, but not VD, was represented in both OCTA-based and multimodal models.

Model	LASSO-Calculated Significant Variables
Demographic	Age, race, sex
VD-FD	Superficial FD, Deep FD, RPC FD, RPC VD
VLD-FD	Superficial VLD, Deep FD, RPC FD
Clinical	RNFL, CDR, CCT
Multimodal	RPC FD, RNFL, CDR, Race, Sex

Table 4: LASSO regression models.

Fig. 3 shows AUC analysis for all five models: multimodal (0.898), clinical (0.888), VD-FD (0.780), VLD-FD (0.774) and demographic (0.741). The multimodal model was significantly more accurate than the clinical ($p = 0.035$), VD-FD ($p < 0.001$), VLD-FD ($p < 0.001$) and demographic models ($p < 0.001$).

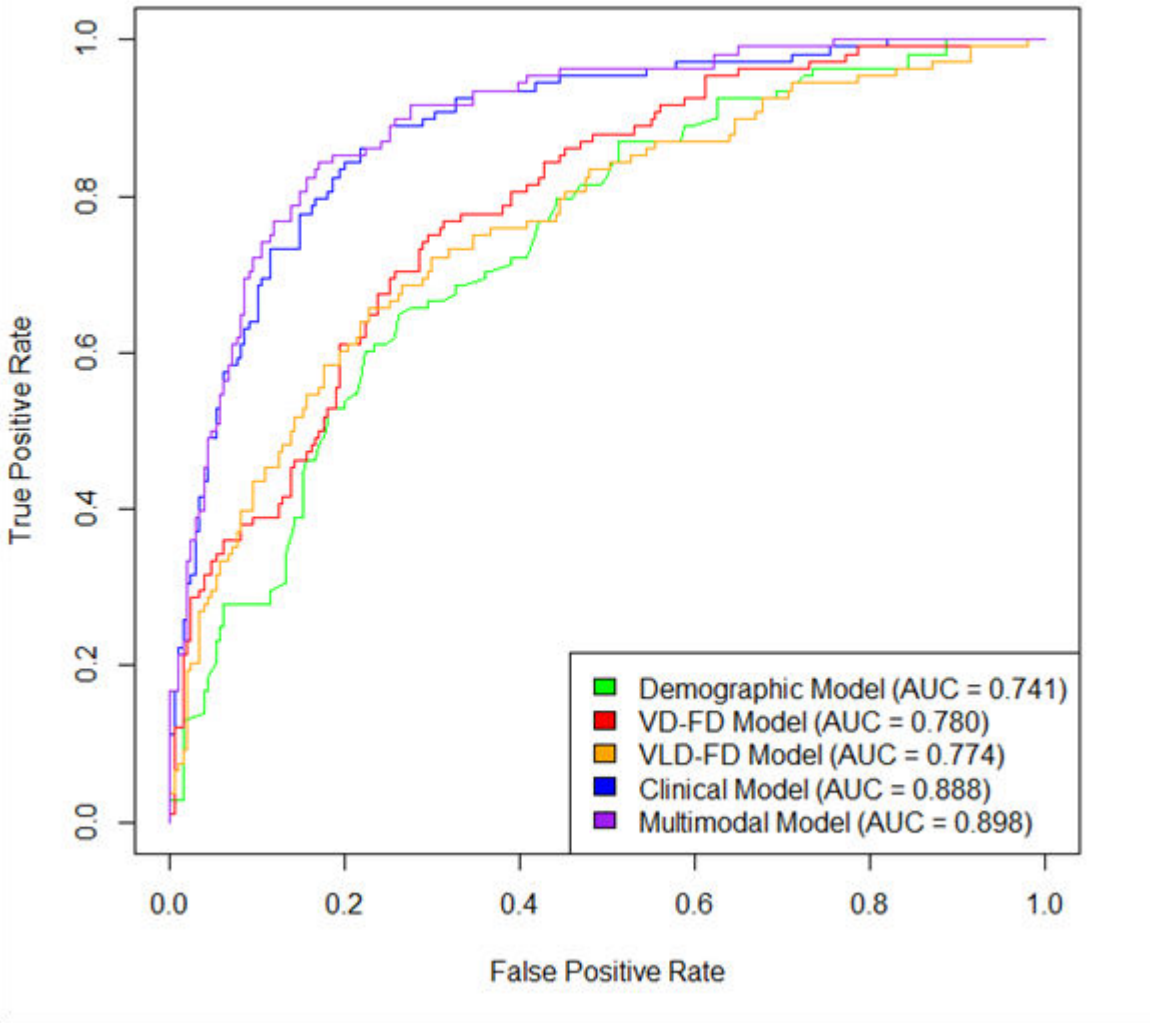

Figure 3: Model AUC analysis.

Discussion

In this study, we analyzed the demographic, clinical and vascular data of 122 POAG and 235 non-POAG patients to characterize the efficacy of multimodal OCTA analysis in glaucoma diagnosis. Significant reductions in OCTA VD, VLD and FD were noted between POAG and non-POAG patients in all scan layers ($p < 0.001$). LASSO regression analysis found that RPC FD was among the most significant variables distinguishing POAG from non-POAG, along with RNFL thickness, CDR, race and sex. Finally, comparison of different diagnostic models demonstrated that a multimodal approach combining OCTA variables with clinical and demographic data performed the best (AUC = 0.898), followed by the clinical data model (AUC = 0.888), the VD-FD model (AUC = 0.780), the VLD-FD model (AUC = 0.774) and the demographic data model (AUC = 0.741).

One major finding from this study is that FD is highly correlated with glaucoma diagnosis, even when including borderline populations such as GS and OHT. LASSO regression strongly favored FD compared to the other OCTA parameters, using FD for ¾ variables in the VD-FD model and 2/3 variables in the VLD-FD model. Furthermore, RPC FD was one of the five variables included in the final multimodal model. Taken together, this data suggests that FD may be superior to VD in diagnosing POAG.

One explanation is that FD is more sensitive to microvascular changes than VD; an analysis of RVO patients before and after a 12-week course of intravitreal bevacizumab showed that FD measurement increased following the treatment, reflecting the improved Best Corrected Visual Acuity (BCVA), while VD continued to decrease [27]. Another possibility is that FD is more sensitive to changes in glaucoma progression (reflecting both mechanical and vascular theories), allowing for better differentiation between POAG and GS. This theory was corroborated by Ciancaglini, et al., who demonstrated that FD was significantly reduced in patients with advanced glaucoma while showing minimal changes in patients with early stage glaucoma [20]. This means that patients with significantly reduced FD are much more likely to have POAG, making it a highly specific marker.

The second goal of this study was to characterize OCTA-based glaucoma diagnosis in a diverse patient population. To date, most studies of OCTA in glaucoma have included only healthy and POAG patients. In contrast, our patient cohort included both GS and OHT, providing a more representative assessment of OCTA's utility in glaucoma diagnosis. Our results demonstrate that OCTA parameters alone may not be as effective as combining them with clinical and structural factors [28,29]. For example, an analysis by Chen, et al., which included healthy, POAG and GS found that RNFL was superior to OCTA VD alone in discriminating healthy from POAG (AUC 0.97 vs 0.82, $p = 0.009$) as well as GS (AUC 0.7 vs 0.6, $p > 0.10$) [29]. Similarly, a study by Chihara, et al., indicates that RNFL performs significantly better than VD when including OHT patients (AUC 0.936 vs 0.832, $p = 0.05$) [28]. While these results understate the importance of OCTA, our combined model suggests a strong utility for OCTA as an important adjunctive tool. Furthermore, the OCTA model's superior performance compared to demographic data suggests that poor vascular perfusion is an important predictor of glaucoma in addition to traditional risk factors such as age, race and ethnicity. This has been supported by previous studies which found low superotemporal peripapillary VD to be associated with POAG progression independent of other factors such as age, sex, RNFL, blood pressure, axial length and IOP [30]. Thus, OCTA provides a wealth of information that can be utilized in borderline or difficult to diagnose cases.

This study has several strengths. First, its 357-patient population makes it one of the largest studies examining OCTA in POAG diagnosis. Second, it is one of the few investigations that include both GS and OHT patients. Third, this investigation included multiple different OCTA parameters, allowing for quantification of both the quantity and quality of patient vasculature. Fourth, the study's usage of LASSO regression allowed us to discern which specific OCTA parameters and clinical variables were most effective in diagnosing glaucoma. Finally, the diverse, multiethnic patient population may provide the basis for future generalizable conclusions.

This study also had several limitations. First, to maximize the sample size, we included both eyes, which may have limited the rigor of our statistical inquiry. Second, as our data was collected from a study period of over 2 years, device and software updates may have affected vascular measurements. Third, LASSO regression may exclude some significant factors due to its tendency to minimize the number of predictors. Fourth, this study did not compare differences between glaucoma severities. Finally, our study utilized 1-fold cross validation; 5- or 10-fold validation would reduce model variability.

Conclusion

In conclusion, our analysis of healthy, GS, OHT and POAG eyes demonstrated that OCTA is an excellent additional tool for glaucoma diagnosis. FD in particular was identified as a promising novel metric for studying microvascular changes in glaucoma.

Conflict of Interest Statement

The authors declare no potential conflicts of interest with respect to the research, authorship, and/or publication of this article.

Acknowledgement

Not applicable

Funding Details

Funded in part by NIH/NEI Core Grant for Vision Research P30EY030413 and a Challenge Grant from Research to Prevent Blindness, New York, NY.

Ethical Approval and Consent to Participate

Ethical approval was obtained from the UT Southwestern Medical Center Institutional Review Board (IRB number STU 052011-145). Informed consent requirement was waived for the purposes of this study.

Data Availability

All data is available from the authors upon reasonable request.

References

1. Allison K, Patel D, Alabi O. Epidemiology of glaucoma: The past, present and predictions for the future. Cureus. 2020;12(11):e11686.
2. Weinreb RN, Aung T, Medeiros FA. The pathophysiology and treatment of glaucoma: A review. JAMA. 2014;311(18):1901-11.
3. Feng KM, Tsung TH, Chen YH, Lu DW. The role of retinal ganglion cell structure and function in glaucoma. Cells. 2023;12(24).
4. Müller H. Anatomische beiträge zur ophthalmologie. Arch Für Ophthalmol. 1858;4(2):1-54.
5. Graefe V. Amaurose mit sehnervenexcavation. Arch Ophthalmol. 1857;3:484.
6. Jaeger E. Ueber glaucom und seine Heilung durch Iridectomie. Wien: Druck von C. Gerold's Sohn. 1858.
7. Wang X, Wang M, Liu H, et al. The association between vascular abnormalities and glaucoma-what comes first? Int J Mol Sci. 2023;24(17).
8. Wollstein G, Kagemann L, Bilonick RA. Retinal nerve fibre layer and visual function loss in glaucoma: The tipping point. Br J Ophthalmol. 2012;96(1):47-52.
9. Rao HL, Pradhan ZS, Suh MH, Moghimi S, Mansouri K, Weinreb RN. Optical coherence tomography angiography in glaucoma. J Glaucoma. 2020;29(4):312-21.
10. WuDunn D, Takusagawa HL, Sit AJ. OCT angiography for the diagnosis of glaucoma: Aa report by the American Academy of Ophthalmology. Ophthalmology. 2021;128(8):1222-35.
11. Kalva P, Akram R, Mekala P, Patel M, Suresh S, Kooner KS. Quantification of vascular morphology in optical coherence tomography angiography in primary open-angle glaucoma. Adv Ophthalmol Pract Res. 2023;3(3):119-25.
12. Rao HL, Pradhan ZS, Weinreb RN. A comparison of the diagnostic ability of vessel density and structural measurements of optical coherence tomography in primary open-angle glaucoma. PLoS One. 2017;12(3):e0173930.
13. Geyman LS, Garg RA, Suwan Y. Peripapillary perfused capillary density in primary open-angle glaucoma across disease stage: an optical coherence tomography angiography study. Br J Ophthalmol. 2017;101(9):1261-8.
14. Lu P, Xiao H, Liang C, Xu Y, Ye D, Huang J. Quantitative analysis of microvasculature in macular and peripapillary regions in early primary open-angle glaucoma. Curr Eye Res. 2020;45(5):629-35.
15. Bhagat PR, Deshpande KV, Natu B. Utility of ganglion cell complex analysis in early diagnosis and monitoring of glaucoma using a different spectral domain optical coherence tomography. J Curr Glaucoma Pract. 2014;8(3):101-6.
16. Scuderi G, Fragiotta S, Scuderi L, Iodice CM, Perdicchi A. Ganglion cell complex analysis in glaucoma patients: What can it tell us? Eye Brain. 2020;12:33-44.
17. Liew G, Gopinath B, White AJ, Burlutsky G, Yin Wong T, Mitchell P. Retinal vasculature fractal and stroke mortality. Stroke. 2021;52(4):1276-82.
18. Kamalipour A, Moghimi S, Khosravi P. Combining optical coherence tomography and optical coherence tomography angiography longitudinal data for the detection of visual field progression in glaucoma. Am J Ophthalmol. 2023;246:141-54.
19. Kwon HJ, Kwon J, Sung KR. Additive role of optical coherence tomography angiography vessel density measurements in glaucoma diagnoses. Korean J Ophthalmol. 2019;33(4):315-25.
20. Ciancaglini M, Guerra G, Agnifili L. Fractal dimension as a new tool to analyze optic nerve head vasculature in primary open-angle glaucoma. In Vivo. 2015;29(2):273.
21. Li Z, Xu Z, Liu Q, Chen X, Li L. Comparisons of retinal vessel density and glaucomatous parameters in optical coherence tomography angiography. PLoS One. 2020;15(6):e0234816.
22. Song C, Kim S, Lee K. Fractal dimension of peripapillary vasculature in primary open-angle glaucoma. Korean J Ophthalmol. 2022;36.
23. Song Y, Cheng W, Li F. Ocular factors of fractal dimension and blood vessel tortuosity derived from OCTA in a healthy

Chinese population. Transl Vis Sci Technol. 2022;11(5):1.
24. Ahmad SS. Glaucoma suspects: a practical approach. Taiwan J Ophthalmol. 2018;8(2):74-81.
25. Yousefi J. Image binarization using Otsu thresholding algorithm. 2015.
26. Panigrahy C, Seal A, Mahato NK, Bhattacharjee D. Differential box counting methods for estimating fractal dimension of gray-scale images: A survey. Chaos Solitons Fractals. 2019;126:178-202.
27. Abdelsalam DT, El Sanabary Z, Hassan N, Soliman M. Comparison between post-treatment vascular density, fractal dimension and choriocapillaris flow in ischemic and non-ischemic retinal vein occlusion using optical coherence tomography angiography. Int J Health Sci. 2022;6(S6):177-90.
28. Chihara E, Dimitrova G, Amano H, Chihara T. Discriminatory power of superficial vessel density and prelaminar vascular flow index in eyes with glaucoma and ocular hypertension and normal eyes. Invest Ophthalmol Vis Sci. 2017;58(1):690-7.
29. Chen CL, Zhang A, Bojikian KD. Peripapillary retinal nerve fiber layer vascular microcirculation in glaucoma using optical coherence tomography-based microangiography. Invest Ophthalmol Vis Sci. 2016;57(9):75-85.
30. Wang YM, Shen R, Lin TPH. Optical coherence tomography angiography metrics predict normal tension glaucoma progression. Acta Ophthalmol. 2022;100(7):e1455-62.